Author Manuscript

Author Manuscript

Author Manuscript

Author Manuscript

HHS Public Access

Author manuscript

Circ Cardiovasc Genet. Author manuscript; available in PMC 2016 October 01.

Published in final edited form as:

Circ Cardiovasc Genet. 2015 October ; 8(5): 653–664. doi:10.1161/CIRCGENETICS.114.000957.

In vivo Analysis of Troponin C Knock-in (A8V) Mice: Evidence that *TNNC1* Is a Hypertrophic Cardiomyopathy Susceptibility Gene

Adriano S. Martins, PhD[#1], **Michelle S. Parvatiyar, PhD**[#2,10], **Han-Zhong Feng, MD, PhD**[3], **J. Martijn Bos, MD, PhD**[4], **David Gonzalez-Martinez**[1], **Milica Vukmirovic, PhD**[1], **Rajdeep S. Turna, MS**[1], **Marcos A. Sanchez-Gonzalez, MD, PhD**[1,5], **Crystal-Dawn Badger, BS**[1], **Diego A. R. Zorio, PhD**[6], **Rakesh K. Singh, PhD**[7], **Yingcai Wang, MD, PhD**[2], **J.-P. Jin, MD, PhD**[3], **Michael J. Ackerman, MD, PhD**[4,8,9], and **Jose R. Pinto, PhD**[1]

[1]Department of Biomedical Sciences, College of Medicine, Florida State University, Tallahassee

[2]Department of Molecular and Cellular Pharmacology, University of Miami, Miller School of Medicine, Miami, FL

[3]Department of Physiology, Wayne State University School of Medicine, Detroit, MI

[4]Department of Molecular Pharmacology & Experimental Therapeutics, Windland Smith Rice Sudden Death Genomics Laboratory, Mayo Clinic, Rochester, MN

[5]Department of Biomedical Sciences, Larkin Health Sciences Institute, South Miami, FL

[6]Department of Chemistry & Biochemistry, College of Medicine, Florida State University, Tallahassee

[7]Translational Science Laboratory, College of Medicine, Florida State University, Tallahassee

[8]Department of Medicine/Division of Cardiovascular Diseases, Mayo Clinic, Rochester, MN

[9]Department of Pediatrics/Division of Pediatric Cardiology, Mayo Clinic, Rochester, MN

[#] These authors contributed equally to this work.

Abstract

Background—Mutations in thin-filament proteins have been linked to hypertrophic cardiomyopathy (HCM), but it has never been demonstrated that variants identified in the *TNNC1* (gene encoding troponin C) can evoke cardiac remodeling *in-vivo*. The goal of this study was to determine whether *TNNC1* can be categorized as an HCM susceptibility gene, such that a mouse model can recapitulate the clinical presentation of the proband.

Correspondence: Jose Renato Pinto, PhD, Department of Biomedical Sciences, College of Medicine, Florida State University, Room 1350-H, 1115 West Call Street, Tallahassee, FL, 32306-4300, Tel: (850) 645-0016, Fax: (850) 644-9399, jose.pinto@med.fsu.edu.
[10]Present Address: Department of Integrative Biology and Physiology, University of California, Los Angeles, CA

Conflict of Interest Disclosures: MJA is a consultant for Boston Scientific, Gilead Sciences, Medtronic, and St. Jude Medical and also receives royalties from Transgenomic for FAMILION-LQTS and FAMILION-CPVT testing. However, none of these companies had anything to do with this study.

Author Manuscript Author Manuscript Author Manuscript Author Manuscript

Methods and Results—The TNNC1-A8V proband diagnosed with severe obstructive HCM at 34-years of age exhibited mild-to-moderate thickening in left and right ventricular walls, decreased left-ventricular dimensions, left-atrial enlargement and hyperdynamic left-ventricular systolic function. Genetically-engineered knock-in mice containing the A8V mutation (heterozygote=KI-TnC-A8V$^{+/-}$; homozygote=KI-TnC-A8V$^{+/+}$) were characterized by echocardiography and pressure-volume studies. Three-month-old, KI-TnC-A8V$^{+/+}$ mice displayed decreased ventricular dimensions, mild diastolic dysfunction, and enhanced systolic function, while KI-TnC-A8V$^{+/-}$ mice displayed cardiac restriction at 14-months of age. KI hearts exhibited atrial enlargement, papillary-muscle hypertrophy and fibrosis. Liquid chromatography-mass spectroscopy was used to determine incorporation of mutant cTnC (~21%) into the KI-TnC-A8V$^{+/-}$ cardiac myofilament. Reduced diastolic sarcomeric length, increased shortening and prolonged Ca^{2+} and contractile transients were recorded in intact KI-TnC-A8V$^{+/-}$ and KI-TnC-A8V$^{+/+}$ cardiomyocytes. Ca^{2+}-sensitivity of contraction in skinned fibers increased with mutant gene dose: KI-TnC-A8V$^{+/+}$ > KI-TnC-A8V$^{+/-}$ > WT, while KI-TnC-A8V$^{+/+}$ relaxed more slowly upon flash-photolysis of diazo-2.

Conclusions—The TNNC1-A8V mutant increases the Ca^{2+}-binding affinity of the thin filament, and elicits changes in Ca^{2+} homeostasis and cellular remodeling, which leads to diastolic dysfunction. These *in-vivo* alterations further implicate the role of *TNNC1* mutations in the development of cardiomyopathy.

Keywords

cardiomyopathy; troponin; mouse; calcium sensitization; myofilament protein; hypertrophic cardiomyopathy; TNNC1; knock-in mouse model; Ca handling; troponin C

When intracellular Ca^{2+} levels saturate cardiac troponin C's (cTnC) single low-affinity regulatory Ca^{2+}-binding site II, a series of conformational changes occur amongst the proteins that make up the thin filament, allowing myosin to cycle faster with actin, thus leading to force generation.[1] Troponin C is part of a regulatory trimeric protein troponin complex (Tn) situated at regular intervals along the thin filament. Tn is also comprised of Troponin I (TnI), which inhibits crossbridge formation between myosin and actin, and Troponin T (TnT) which is important for myofilament activation and anchoring of the Tn complex to the thin filament.[2, 3] Fluctuations in intracellular Ca^{2+} during excitation-contraction coupling control the contractile and relaxation phases of cardiac contraction.[1] Hence, perturbations in the Ca^{2+} affinity of cTnC can modify myofilament function, as demonstrated by *in vitro* studies.[4, 5]

In an effort to determine whether the *TNNC1* (cTnC gene) might be associated with HCM, a large cohort of unrelated HCM patients was screened for mutations, which revealed the existence of four rare cTnC variants.[6] Recently, two other *TNNC1* mutations have been identified in HCM patients.[7, 8] Direct evidence that points toward causality for these mutations is lacking. The absence of positive family history of HCM disease or comprehensive linkage analysis has hindered the designation of *TNNC1* as an established HCM-susceptibility gene.[6] Therefore, what has remained elusive is an established link between the variants found in *TNNC1* and the disease processes that lead to the development of HCM.

Author Manuscript Author Manuscript Author Manuscript Author Manuscript

Our laboratory has used *in-vitro* tools to define cTnC variants as disease-causing by assaying for functional changes and determining whether they fit within parameters of known, established pathogenic thin filament HCM mutations.[6, 9, 10] In this regard, a rare heterozygote variant A8V in *TNNC1* was identified in an HCM patient who was genotype negative for mutations in eight other sarcomeric protein genes.[6] The substitution of alanine for valine at position 8 in cTnC is located in the N-helix, which is known to modulate Ca^{2+}-binding affinity of both the C- and N-terminal domains.[11, 12] Assessments were made as to whether cTnC-A8V led to disease-like properties in functional tests that included porcine skinned fibers and reconstituted actomyosin ATPase assays.[6, 9] In reconstituted functional assays, the cTnC-A8V mutant demonstrated an ability to sensitize the myofilament to Ca^{2+}.[6, 9] Although this compilation of findings strongly suggested that the cTnC-A8V mutant was the cause of HCM in the patient, additional proof was still necessary. The proband had a negative family history of HCM and therefore the rare variant could not be shown to segregate with the disease.

Here, we describe the functional consequences of the first cTnC animal model generated to date, a mouse bearing the mutation A8V inserted via a knock-in strategy. As in the TNNC1-A8V proband, the knock-in mouse containing the cTnC-A8V (KI-TnC-A8V) also developed mild to moderate left- and right-ventricular hypertrophy, hyperdynamic systolic function and atrial enlargement. Furthermore, we explored the underlying cellular and molecular mechanisms governing the disease process in the KI-TnC-A8V mice. Altered mechanical function and Ca^{2+} handling in intact cardiomyocytes were accompanied by increased Ca^{2+} sensitivity of contraction, likely contributing to cardiac dysfunction. Profound clinical similarities regarding the manifestation of disease in the patient and animal model provide evidence that increased cTnC N-domain Ca^{2+} affinity is an underlying mechanism of HCM and that TNNC1-A8V is a definite HCM-causative mutation. Altogether, these findings further establish that *TNNC1* is a HCM susceptibility gene.

Methods

For further details, see Supplemental methods.

Clinical data

The proband presented to Mayo Clinic for clinical evaluation and management of HCM and consented to participate in an IRB-approved protocol.[6]

Mice

All protocols and experimental procedures followed NIH guidelines and were approved by University of Miami, Florida State University and Wayne State University Animal Care and Use Committee (ACUC).

Statistical Analysis

All values are presented as mean ± S.E. Significance for echocardiography (ECHO), gene expression levels, Ca^{2+} and contractile transients in intact cardiomyocytes, Ca^{2+} sensitivity of contraction and flash photolysis in skinned fibers and immunoblot data were determined

Author Manuscript Author Manuscript Author Manuscript Author Manuscript

by one-way ANOVA using Fisher LSD or Bonferroni post-hoc analysis. Significance for body weight, heart/body weight, atrial weight, atrial/heart weight were determined by one-way ANOVA with Tukey post-hoc analysis, while two-way or one-way ANOVA with Tukey post-hoc analysis was used for pressure-volume (P-V) studies depending on the comparison indicated in the Figure legend 2. A priori alpha level of $p < 0.05$ was considered to be significant.

Results

Clinical presentation of the patient with the TNNC1-A8V mutation

The proband was first examined at the Mayo Clinic in 2003 and after consenting to a study, was found to be genotype positive for the rare missense A8V-variant in *TNNC1*. Clinically, he was diagnosed with severe obstructive HCM at age 34 exhibiting increased left and right ventricular wall thickness and a left ventricular outflow tract gradient of 117 mm HG at rest with systolic anterior motion of the mitral valve. An ECHO (Figure 1A and B) was performed indicating: 1) increased ventricular septal thickness of 28 mm (normal value: 9-12 mm) and posterior wall thickness of 15 mm (normal value: 8-12 mm); 2) decreased left ventricular dimensions 38 mm (normal value: 43-57 mm) during the diastolic interval and 21 mm (normal value: 26-37 mm) during the systolic interval; 3) mild-moderate left atrial enlargement (end-diastolic dimension 49 mm (normal value: 31-45 mm), left atrium volume 40 cc/mm^2 (normal value: 17-27 cc/mm^2)); and 4) hyperdynamic left ventricular systolic function (calculated ejection fraction (EF) 73%). ECG-tracings obtained during the following years of evaluation (2003-2005; Figures 1 C-G) showed evidence of myocardial ischemia, left ventricular hypertrophy and left atrial enlargement. The patient had a negative family history for HCM or sudden cardiac death after genetic testing of his parents, grandparents and members of his extended family. At the time of his diagnosis (2003), the proband had 2 sons, ages 12 and 14 who were asymptomatic and clinically negative for HCM by screening ECHO. Over time, the proband's symptoms progressed to NYHA Class III with chest pain, dyspnea on exertion and light headedness and in May of 2004, he underwent surgical septal myectomy. Based on the severity of disease, an implantable cardioverter defibrillator was implanted in October of 2004. A 24h-Holter recording during this time showed a sinus rhythm with a wandering atrial pacemaker, with the rate varying from 61 to 109 bpm. The patient and his sons have not been seen at the Mayo Clinic since 2005.

Echocardiography of KI-TnC-A8V mice

The KI mice were analyzed by ECHO to determine how the cTnC-A8V variant affected cardiac function in mice at 3, 9, and 14 months (m) of age. A representative M-mode image of the left ventricle from a 14m-old KI-TnC-A8V$^{+/+}$ mouse heart is shown in Figure 2B, in which a narrowing of the cardiac chamber lumen can be observed compared to age-matched WT (Figure 2A). The end diastolic volume (EDV, μl), end systolic volume (ESV) and left ventricular dimensions were reduced significantly in KI-TnC-A8V$^{+/+}$ at all ages tested. For KI-TnC-A8V$^{+/-}$, left ventricular dimensions were significantly reduced only at 14m compared to WT (See Table 1). Since KI mouse hearts may undergo changes in size, we attempted to calculate relative wall thickness (RWT). As shown in Table 1, significant

Author Manuscript Author Manuscript Author Manuscript Author Manuscript

changes in RWT can be observed in KI-TnC-A8V$^{+/-}$ and KI-TnC-A8V$^{+/+}$ hearts as early as 3m compared to WT. The EF was increased in KI-TnC-A8V$^{+/+}$ mice at 3 and 9m of age, suggesting hyperdynamic left-ventricular systolic function that was also seen in the patient (Table 1). The isovolumic contraction time was found decreased for the KI-TnC-A8V$^{+/+}$ mice at 9 and 14m of age. Additional changes occurred in parameters related to diastolic function (increased isovolumic relaxation time and decreased mitral valve early peak flow velocity/atrial peak flow velocity (MV E/A)) for KI-TnC-A8V$^{+/+}$ at different ages, consistent with Stage I diastolic dysfunction. Clinical findings from the patient indicated an MV E/A ratio of 1.13 (normal values 0.9-2.5) in an ECHO performed in 2003.

Pressure-Volume (P-V) studies of KI-TnC-A8V mice

Cardiac function was examined in *ex-vivo* working heart preparations at baseline and 3, 10 or 30 nM isoproterenol (ISO) in 12-13m-old mice. Higher stroke volumes (SV) were seen when normalized to heart weight in KI-TnC-A8V$^{+/+}$ and KI-TnC-A8V$^{+/-}$ compared to WT hearts (Fig. 2C), indicating augmented systolic function. KI-TnC-A8V$^{+/-}$ hearts had higher LVP_{max} values compared to WT and KI-TnC-A8V$^{+/+}$ (Fig. 2D), while the KI-TnC-A8V$^{+/+}$ hearts displayed higher LVP_{min} values compared to KI-TnC-A8V$^{+/-}$ (Fig. 2E). The diastolic velocity (–dP/dt) of KI-TnC-A8V$^{+/+}$ hearts was decreased compared to WT and KI-TnC-A8V$^{+/-}$ (Fig. 2G). Examination of baseline cardiac function revealed higher LVP_{min} values in KI-TnC-A8V$^{+/+}$ compared to KI-TnC-A8V$^{+/-}$ and lower –dP/dt in KI-TnC-A8V$^{+/+}$ compared to KI-TnC-A8V$^{+/-}$ and WT hearts, indicating impaired diastolic function (Figure 2E and G). The systolic velocity (+dP/dt) of KI-TnC-A8V$^{+/+}$ and KI-TnC-A8V$^{+/-}$ hearts were similar to WT (Figure 2F).

Heart weight of KI-TnC-A8V mice

In 12-13m-old mice, no significant difference was found in the body weight (BW) of KI-TnC-A8V$^{+/-}$ and KI-TnC-A8V$^{+/+}$ compared to WT (Figure 3A). However, the heart weight (HW) to BW ratio (HW/BW) was significantly reduced in both KI-TnC-A8V$^{+/-}$ and KI-TnC-A8V$^{+/+}$ mice (Figure 3B). Left atrial (LA) mass in KI-TnC-A8V$^{+/+}$ mice was dramatically increased as shown by the increased weight of the LA alone and when compared to the whole heart weight LA/HW ratio compared to WT hearts (Figure 3C and D), suggesting adaptive remodeling occurred in response to impaired left-ventricular diastolic function. No significant changes were observed in the right atria of these mice (data not shown).

Cardiac fetal gene expression in mutant KI-TnC-A8V mice

Consistent with the previous findings indicating occurrence of a cardiomyopathic process, mRNA expression levels of brain natriuretic peptide (BNP) and atrial natriuretic peptide (ANP) by qRT-PCR were significantly increased in the left ventricle of 16-18m KI-TnC-A8V$^{+/+}$ and KI-TnC-A8V$^{+/-}$ mice compared to age-matched controls, while mRNA expression levels of myosin heavy chain β (MHCβ) increased only in the KI-TnC-A8V$^{+/+}$ left ventricle (Figure 3E). In addition, we assessed the expression levels of fetal genes in the right ventricle. Only KI-TnC-A8V$^{+/+}$ mice showed a significant increase in BNP and ANP gene expression compared to WT (Figure 3F).

Author Manuscript Author Manuscript Author Manuscript Author Manuscript

Assessment of histopathology in KI-TnC-A8V hearts

The hearts of 16-18m-old mice were stained using Masson trichome and evaluated for changes in tissue architecture and fibrosis. Representative images are shown in Figure 4 and the black arrows indicate the location of the papillary muscle. Compared to WT (Panels A and D), the hearts of KI-TnC-A8V$^{+/-}$ (Panels B and E) and KI-TnC-A8V$^{+/+}$ (Panels C and F) exhibited papillary muscle hypertrophy as well as interstitial fibrosis, consistent with findings of HCM. In addition, myofibrillar disarray, atrial enlargement, right ventricular wall and apical hypertrophy were observed in both KI-TnC-A8V$^{+/-}$ and KI-TnC-A8V$^{+/+}$ hearts as shown in Supplemental Figure 2A-I.

Determination of mutant to WT protein ratio in the KI-TnC-A8V$^{+/-}$ hearts

Since we are studying KI mice with either one or two alleles mutated, we attempted to determine the ratio of mutant to WT cTnC protein incorporated into the KI-TnC-A8V$^{+/-}$ hearts. Heart extract samples of 4m-old mice were resolved by 15% SDS-PAGE, the cTnC band was excised and extracted from the SDS-PAGE gel, followed by trypsinization. The samples were then analyzed by liquid chromatography mass spectrometry quantification (see supplemental methods for further details). Cardiac TnC was digested at the carboxy-termini of lysine 6 and 17 or 21. Both peptides one of 11 amino acids and the other of 15 amino acids contain the residue number 8 of cTnC. Figure 4G shows the retention time for the different peptides generated by cTnC trypsinization of the WT, KI-TnC-A8V$^{+/-}$ and KI-TnC-A8V$^{+/+}$ heart samples. The graphs show that the ratio quantified by the two peptides yielded the same result, 21.05 ± 1.45% (15 amino acid peptide) and 21.45 ± 1.15% (11 amino acid peptide) of the cTnC-A8V incorporated in the KI-TnC-A8V$^{+/-}$ hearts.

Sarcomere length and intracellular Ca^{2+} levels in intact cardiomyocytes from KI-TnC-A8V mice

Intact cardiomyocytes were isolated from 3m WT, KI-TnC-A8V$^{+/-}$ and KI-TnC-A8V$^{+/+}$ mouse hearts and the intracellular Ca^{2+} and sarcomere length (SL) parameters were recorded at four different stimulation frequencies (1, 2, 4 and 6Hz). From these experiments, we sought to understand how hemodynamics were changed and whether function was impaired at the cellular level, due to the incorporation of mutant cTnC into the myofilament. Figure 5A shows that diastolic SL was significantly shorter in KI-TnC-A8V$^{+/-}$ and KI-TnC-A8V$^{+/+}$ cardiomyocytes compared to WT, at all stimulation frequencies. Next, we evaluated the contractility percentage, and found that the cTnC-A8V mutation present in both KI-TnC-A8V$^{+/-}$ and KI-TnC-A8V$^{+/+}$ cardiac myocytes contributed to an increased contractile percentage (%) at all frequencies of stimulation (Figure 5B). This finding is consistent with the hypercontractile phenotype as evidenced by the increased SV for (KI-TnC-A8V$^{+/-}$ and KI-TnC-A8V$^{+/+}$) and EF for (KI-TnC-A8V$^{+/+}$), reported in Figure 2C and Table 1. Further measurements were conducted to determine resting intracellular Ca^{2+} levels, as monitored by Fura-2AM. It was found that KI-TnC-A8V$^{+/-}$ cardiomyocytes possess higher diastolic Ca^{2+} levels at all pacing frequencies compared to age-matched WT cardiomyocytes, while KI-TnC-A8V$^{+/+}$ showed lower diastolic Ca^{2+} levels only at 6Hz (Figure 5C). Furthermore, the peak Ca^{2+} to baseline measured as a %, was significantly diminished in both KI-TnC-

Author Manuscript Author Manuscript Author Manuscript Author Manuscript

A8V$^{+/-}$ and KI-TnC-A8V$^{+/+}$ cardiomyocytes compared to WT, as shown in Figure 5D. The gene-dosage effect however, is evident in the diastolic SL and peak Ca^{2+} measurements.

Kinetics of SL shortening and Ca^{2+} transient in intact cardiomyocytes from KI-TnC-A8V

To further understand the cellular mechanisms underlying development of HCM elicited by introduction of the cTnC-A8V mutant in mice, we evaluated the kinetics of SL shortening and intracellular Ca^{2+} transients in isolated cardiomyocytes (the representative raw and normalized data traces are shown in Supplemental Figure 3A). This experiment allowed us to investigate the effects of the mutant in an intact cellular system, without the complications of autonomic modulation. The experiment was conducted and recorded using a range of frequencies, from 1 to 6Hz. In Figure 6A and 6B, the SL shortening and intracellular Ca^{2+} kinetics parameters were recorded using two higher pacing frequencies (4 and 6HZ), to evoke outcomes more consistent with cardiac mouse physiology. As shown in Figure 6A (top panels), the T_{50} relaxation time (RT) is determined to be 50% of the time it takes for the SL to return from peak to baseline and was prolonged in KI-TnC-A8V$^{+/-}$ and KI-TnC-A8V$^{+/+}$ cardiomyocytes at 4 and 6Hz stimulation frequencies compared to WT. Note that at 4Hz, the T_{50} RT for SL in KI-TnC-A8V$^{+/+}$ cardiomyocytes was also significantly prolonged compared to KI-TnC-A8V$^{+/-}$. These results suggest that the kinetics of cardiomyocyte relaxation were affected in a gene-dose dependent fashion. The rates of cell re-lengthening at 4 and 6Hz were consistent with results obtained for T_{50} RT, excluding the possibility that a delay in SL relaxation could be caused by excessive cell shortening (Figure 6A, middle panels). The SL shortening time from baseline to peak was found to be significantly prolonged in KI-TnC-A8V$^{+/+}$ and KI-TnC-A8V$^{+/-}$ cardiomyocytes at 4 and 6Hz, compared to WT. Note that KI-TnC-A8V$^{+/+}$ cardiomyocytes was also significantly prolonged compared to KI-TnC-A8V$^{+/-}$ at both frequencies (Figure 6A, bottom panels). Next, we investigated whether the slower SL shortening and re-lengthening kinetics found in KI-TnC-A8V cardiomyocytes correlated with changes in the Ca^{2+} transient. The T_{50} for Ca^{2+} decay (50% of the time for the intracellular Ca^{2+} to return from peak to baseline) was found to be significantly delayed in KI-TnC-A8V$^{+/-}$ and KI-TnC-A8V$^{+/+}$ cardiomyocytes at both frequencies of stimulation compared to WT (Figure 6B, top panels). The T_{50} Ca^{2+} decay was affected in a gene-dosage fashion since it was found to be significantly different between cardiomyocytes obtained from KI-TnC-A8V$^{+/-}$ and KI-TnC-A8V$^{+/+}$. The time from baseline to peak for intracellular Ca^{2+} was also investigated and found to be delayed in KI-TnC-A8V$^{+/+}$ cardiomyocytes compared to KI-TnC-A8V$^{+/-}$ and WT cardiomyocytes when paced at 4 and 6Hz (Figure 6B, bottom panels). The SL T_{50} RT was found to be prolonged similarly in both KI-TnC-A8V$^{+/-}$ and KI-TnC-A8V$^{+/+}$ cardiomyocytes when stimulated at lower frequencies compared to WT, while the effect of gene-dosage on the delay in T_{50} of Ca^{2+} decay was also seen at 1Hz. (Supplemental Figure 3B)

Ca^{2+} sensitivity of contraction and rate of relaxation in skinned fibers from KI-TnC-A8V

To evaluate whether the TnC-A8V mutant elicited cellular, morphological, and hemodynamic changes in the heart due to the fundamentally increased Ca^{2+} affinity of the myofilament; the Ca^{2+} sensitivity of force development in papillary skinned fibers obtained from KI-TnC-A8V$^{+/-}$ and KI-TnC-A8V$^{+/+}$ mice were tested at two different ages (4m and 14-16m-old). The 4m-old KI-TnC-A8V$^{+/-}$ (pCa_{50} = 6.01 ± 0.02) and KI-TnC-A8V$^{+/+}$

Author Manuscript Author Manuscript Author Manuscript Author Manuscript

(pCa_{50} = 6.28 ± 0.02) skinned fibers demonstrated significantly increased Ca^{2+} sensitivity of contraction compared to age-matched WT (pCa_{50} = 5.88 ± 0.03), as shown in Figure 7A. The cooperativity of thin filament activation (n_{Hill}) was significantly decreased in the KI-TnC-A8V$^{+/+}$ (n_{Hill} = 1.79 ± 0.06) skinned fibers compared to those from WT (n_{Hill} = 2.59 ± 0.14) and KI-TnC-A8V$^{+/-}$ (n_{Hill} = 2.26 ± 0.14); whereas the n_{Hill} of the KI-TnC-A8V$^{+/-}$ skinned fibers remained unchanged compared to WT (Figure 7A). The same trend of increased Ca^{2+} sensitivity appeared to occur in a gene-dose-dependent fashion when the experiments were conducted with 14-16m old mice. The n_{Hill} from the 14-16m mice also followed the same trend as the 4m group (Supplemental Figure 4). Flashphotolysis of the diazo-2-loaded skinned fibers indicated that the rate of relaxation was significantly slower for KI-TnC-A8V$^{+/+}$ compared to WT (Figure 7B). The rate constants and amplitudes are included in the figure legend.

Immunoblotting for detection of key Ca^{2+}-handling proteins in KI-TnC-A8V hearts

The proteins responsible for loading the sarcoplasmic reticulum (SR) were assessed to determine whether they underwent adjustments in order to maintain cellular Ca^{2+} homeostasis. Figure 7C shows the representative immunoblots for 9m hearts. The rationale for conducting these experiments at this age is to identify early molecular markers for the disease in KI-TnC-A8V$^{+/-}$ mice since morphological changes are still not evident. Sarcoplasmic reticulum Ca^{2+}-ATPase (SERCA2) protein levels were reduced in heart extracts obtained from KI-TnC-A8V$^{+/-}$ and KI-TnC-A8V$^{+/+}$ mice (Figure 7D). The phosphorylation levels of serines 23,24 in cTnI (TnI-P) were also reduced in both KI-TnC-A8V compared to WT, while the phosphorylation levels of Serine 16 in PLN (PLN-P^{Ser16}) were significantly decreased only in KI-TnC-A8V$^{+/+}$ hearts (Figure 7D). The protein levels of phospholamban (PLN-T), calsequestrin (CASQ2) and $Na^{+}Ca^{2+}$-exchanger (NCX1) were found unaltered in KI-TnC-A8V$^{+/-}$ and KI-TnC-A8V$^{+/+}$ heart extracts (Figure 7D). We also looked for changes occurred in protein expression and phosphorylation of SERCA2 and PLN respectively, in younger (4m) and older (16-18m) groups of mice (Supplemental Figure 5). Interestingly, the phosphorylation levels of Threonine 17 in PLN (PLN-P^{Thr17}) were statistically lower in both KI-TnC-A8V$^{+/-}$ and KI-TnC-A8V$^{+/+}$ hearts throughout the three ages tested. The levels of PLN-P^{Ser16} in KI-TnC-A8V$^{+/-}$ hearts were reduced at 4m, unchanged at 9m and again reduced at 16-18m compared to WT, suggesting some adaptation process to disease has occurred by mid-age. In KI-TnC-A8V$^{+/+}$ hearts, the levels of PLN-P^{Ser16} were lower at all the different ages tested. The levels of PLN-T were lower in both KI-TnC-A8V genotypes only at 16-18m, while SERCA2 was lower at 9m and 16-18m (Supplemental Figure 5). These data suggest that decreased levels of SERCA2 and PLN-P^{Thr17} could provide early molecular indicators of disease in KI-TnC-A8V$^{+/-}$ hearts.

Discussion

The objectives of this work were (i) to provide conclusive evidence that *TNNC1* is an uncommon but definitive HCM-susceptibility gene; (ii) to determine whether changes in the N-terminal domain Ca^{2+} binding affinity of cTnC in a knock-in mouse containing the human HCM-associated A8V mutation are sufficient to induce cardiac remodeling that resembles cardiomyopathic human diseases; and (iii) to investigate the cellular and

Author Manuscript Author Manuscript Author Manuscript Author Manuscript

molecular mechanism underlying the morphological changes in the heart and diastolic dysfunction caused by the aforementioned mutation, while correlating all these results with the clinical phenotytpe of the proband. Upon initial evaluation, the proband reported a negative family history of HCM since his children had not developed disease at this point. Therefore, the lack of unambiguous linkage studies for the cTnC variants discovered has thus far prevented the firm establishment of *TNNC1* as an HCM-susceptibility gene. To date, there are seven cTnC mutations described that are associated with HCM, and only two have demonstrated inheritance among family members.[6-8, 13] Due to the lack of co-segregation studies, *in vivo* studies, such as the one presented here, are therefore of utmost importance. Here we report the cardiac phenotype obtained in the first mouse model specifically designed to test the role of *TNNC1* in HCM-associated disease processes.

Similar to the KI-TnC-A8V mouse model presented here, animal models bearing TnT or TnI mutations associated with HCM either had unchanged or decreased HW/BW ratio.[14-17] Although mouse models do not entirely recapitulate human disease processes, some disease traits are still manifested, e.g., diastolic dysfunction and predisposition to arrhythmias.[14, 18, 19] In this study, we attempted to correlate morphological changes in the heart of the human patient with that of the mouse model containing the TNNC1-A8V mutation. The KI-TnC-A8V mouse mirrored the cardiac remodeling seen in the patient, who displayed mild to moderate right and left ventricular hypertrophy and left atrial enlargement as shown by RWT and histopathological studies. Furthermore, the KI mouse developed mild diastolic dysfunction and hyperdynamic left-ventricular function similar to what was observed in the patient (EF = 73%). The data obtained from the TNNC1-A8V mouse model strongly suggest that this variant is indeed a definitive, pathogenic mutation.

Diastolic dysfunction is a clinical hallmark of HCM. Therefore, an important question to address is the source of impaired left-ventricular relaxation. Upon studying the KI-TnC-A8V mouse, we identified interstitial fibrosis and myofibrillar disarray. These changes in tissue organization may contribute to increased stiffness and impaired muscle relaxation in HCM patients.[20] The left atrial enlargement seen in the TNNC1-A8V patient and in the KI mouse suggest that this mutation may also be implicated in the development of an RCM-like phenotype. This mixed phenotype has become acknowledged in the contemporary classification of inherited cardiomyopathy, which highlights the clinical overlap in the presentation of cardiomyopathies such as HCM and RCM, defined previously as distinct clinical entities.[21]

Experiments performed at the cellular level with KI-TnC-A8V cardiomyocytes indicated a delay in mechanical relaxation and intracellular Ca^{2+} decay times. The molecular explanation for this phenomenon may be that the A8V substitution increases the Ca^{2+}-binding affinity of cTnC and consequently delays the Ca^{2+} dissociation rate from the thin filament, which we have previously shown in reconstituted systems.[22, 23] The drastic Ca^{2+} sensitization observed in reconstituted porcine cardiac fibers (+0.36 pCa units) supported our rationale to subsequently develop the KI-TnC-A8V mouse since this cTnC mutant elicited the largest shift in this parameter among the other cTnC HCM mutants tested.[6] Measurements of the Ca^{2+} sensitivity of contraction in the KI-TnC-A8V skinned fibers, recapitulated our previous findings in reconstituted fibers. These data suggest that increased

Author Manuscript Author Manuscript Author Manuscript Author Manuscript

myofilament Ca^{2+} sensitization causes the impaired mechanical relaxation and delayed Ca^{2+} re-uptake times in the intact KI-TnC-A8V cardiomyocytes, thus fitting a common pathogenetic process seen in TnI and TnT models of HCM.[14, 16, 24] More recently, we and others have shown that genetically engineering the myofilament to desensitize it to Ca^{2+} can potentially reverse the aberrant phenotypes associated with HCM and RCM caused by troponin and tropomyosin mutations.[25, 26]

We found that KI-TnC-A8V cardiomyocytes have shortened SLs during diastole and reduced intracellular Ca^{2+} oscilation between diastole and systole These findings led us to hypothesize that under resting conditions the cardiac myofilaments containing cTnC-A8V are pre-activated.[24, 27] Thus only a small increase in intracellular Ca^{2+} levels (lower than normal physiological requirements) is sufficient to trigger muscle activation equivalent to or greater than that occurring during systole, since EF and SL % of contraction in cardiomyocytes were increased. We and others have reported that HCM and RCM troponin mouse models may have a basal activation of contraction under resting conditions in skinned fibers and intact cells. This in turn, impairing the relaxation phase in diastole. [14, 16, 28]

Adjustments to the levels of Ca^{2+} handling proteins at the plasma membrane and the sarcoplasmic reticulum (SR) are known to occur during heart disease. Consistent with other mouse models of HCM, levels of SERCA2 were found to be decreased in the KI-TnC-A8V hearts, suggesting that the SR is unable to properly buffer intracellular Ca^{2+} levels. Therapeutics that increase Ca^{2+} buffering in cardiomyocytes during active disease states such as HCM and RCM have been successfully tested in mouse models.[29, 30] Interestingly, in our study the levels of PLN-P^{Thr17} were found to decrease in KI-TnC-A8V hearts from 4 months of age onwards, while the levels of PLN-P^{Ser16} fluctuated in KI-TnC-$A8V^{+/-}$ mouse hearts at the three ages tested. This suggests that alterations in Ca^{2+} handling due to the mutant cTnC protein may be sensed at a young age and that compensatory measures are well in place by 9m of age, which further assist in regulation of Ca^{2+} homeostasis. However, upon further aging the stress induced by the mutant cTnC protein seems to overwhelm the regulatory compensation, and the SR proteins are once again relied upon as the main assistive mechanism regulating contractile function, whereas bimodal regulation by PLN-P may fine-tune SR Ca^{2+} uptake during progression of disease. Changes in phosphorylation of PLN, cTnI as well as SERCA2 protein levels occur even before visible structural changes are detected in the KI-TnC-$A8V^{+/-}$ heart. The decreased levels of PLN-T seen only at 16-18m may indicate that the disease may have progressed to a more advanced stage and/or a combination of disease and effects of aging. The decreased levels of cTnI-P observed in KI-TnC-A8V mouse hearts is suggested to be a hallmark of the disease process since it was previously found that cardiac samples obtained from HCM patients who harbor mutations in sarcomeric proteins have decreased levels of cTnI-P.[31] The decreased phosphorylation levels of cTnI may be explained by the increased activity of phosphatases seen in patients transitioning into different stages of disease such as heart failure.[32]

Herein, we describe the functional consequences of the first cTnC animal model generated to date, a mouse that bears the human heterozygous mutation A8V inserted via a knock-in strategy. The heterozygote and homozygote mice displayed functional and morphological changes that were consistent overall with the HCM phenotype, presenting a striking

Author Manuscript Author Manuscript Author Manuscript Author Manuscript

correlation to the phenotype of the human proband. In conclusion, this study provides compelling evidence that mutation in *TNNC1* is a pathogenic mechanism that underlies the development of HCM.

Supplementary Material

Refer to Web version on PubMed Central for supplementary material.

Acknowledgments

The authors thank Ana Rojas, Edda Ruiz, Jingsheng Liang and Brittany Griffin for the technical and animal husbandry assistance. The LCMS experiment was carried out in the Translational Science Laboratory, FSU College of Medicine. The authors would like to thank Dr. Roger Mercer, Director of Translational Science Laboratory for providing rapid and efficient service.

Funding Sources: This research was supported by National Heart, Lung and Blood Institute of the National Institutes of Health Grant HL103840 to JRP, HL098945 to JPJ, AHA Postdoctoral Fellowship 09POST2300030 to MSP, Florida Heart Research Institute to JRP and the Mayo Clinic Windland Smith Rice Comprehensive Sudden Cardiac Death Program to MJA. JRP acknowledges generous start-up support from the FSU College of Medicine.

References

1. Gordon AM, Homsher E, Regnier M. Regulation of contraction in striated muscle. Physiol Rev. 2000; 80:853–924. [PubMed: 10747208]
2. Takeda S, Yamashita A, Maeda K, Maeda Y. Structure of the core domain of human cardiac troponin in the Ca(2+)-saturated form. Nature. 2003; 424:35–41. [PubMed: 12840750]
3. Farah CS, Reinach FC. The troponin complex and regulation of muscle contraction. Faseb J. 1995; 9:755–767. [PubMed: 7601340]
4. Parvatiyar MS, Pinto JR, Liang J, Potter JD. Predicting cardiomyopathic phenotypes by altering Ca2+ affinity of cardiac troponin C. J Biol Chem. 2010; 285:27785–27797. [PubMed: 20566645]
5. Tikunova SB, Davis JP. Designing calcium-sensitizing mutations in the regulatory domain of cardiac troponin C. J Biol Chem. 2004; 279:35341–35352. [PubMed: 15205455]
6. Landstrom AP, Parvatiyar MS, Pinto JR, Marquardt ML, Bos JM, Tester DJ, et al. Molecular and functional characterization of novel hypertrophic cardiomyopathy susceptibility mutations in TNNC1-encoded troponin C. J Mol Cell Cardiol. 2008; 45:281–288. [PubMed: 18572189]
7. Chung WK, Kitner C, Maron BJ. Novel frameshift mutation in Troponin C (TNNC1) associated with hypertrophic cardiomyopathy and sudden death. Cardiol Young. 2011; 21:345–348. [PubMed: 21262074]
8. Parvatiyar MS, Landstrom AP, Figueiredo-Freitas C, Potter JD, Ackerman MJ, Pinto JR. A Mutation in TNNC1-encoded Cardiac Troponin C, TNNC1-A31S, Predisposes to Hypertrophic Cardiomyopathy and Ventricular Fibrillation. J Biol Chem. 2012; 287:31845–31855. [PubMed: 22815480]
9. Pinto JR, Parvatiyar MS, Jones MA, Liang J, Ackerman MJ, Potter JD. A functional and structural study of troponin C mutations related to hypertrophic cardiomyopathy. J Biol Chem. 2009; 284:19090–19100. [PubMed: 19439414]
10. Willott RH, Gomes AV, Chang AN, Parvatiyar MS, Pinto JR, Potter JD. Mutations in Troponin that cause HCM, DCM AND RCM: what can we learn about thin filament function? J Mol Cell Cardiol. 2010; 48:882–892. [PubMed: 19914256]
11. Smith L, Greenfield NJ, Hitchcock-DeGregori SE. Mutations in the N- and D-helices of the N-domain of troponin C affect the C-domain and regulatory function. Biophys J. 1999; 76:400–408. [PubMed: 9876151]
12. Chandra M, da Silva EF, Sorenson MM, Ferro JA, Pearlstone JR, Nash BE, et al. The effects of N helix deletion and mutant F29W on the Ca2+ binding and functional properties of chicken skeletal muscle troponin. J Biol Chem. 1994; 269:14988–14994. [PubMed: 8195134]

Author Manuscript Author Manuscript Author Manuscript Author Manuscript

13. Hoffmann B, Schmidt-Traub H, Perrot A, Osterziel KJ, Gessner R. First mutation in cardiac troponin C, L29Q, in a patient with hypertrophic cardiomyopathy. Hum Mutat. 2001; 17:524. [PubMed: 11385718]
14. Tardiff JC, Hewett TE, Palmer BM, Olsson C, Factor SM, Moore RL, et al. Cardiac troponin T mutations result in allele-specific phenotypes in a mouse model for hypertrophic cardiomyopathy. J Clin Invest. 1999; 104:469–481. [PubMed: 10449439]
15. Hernandez OM, Szczesna-Cordary D, Knollmann BC, Miller T, Bell M, Zhao J, et al. F110I and R278C troponin T mutations that cause familial hypertrophic cardiomyopathy affect muscle contraction in transgenic mice and reconstituted human cardiac fibers. J Biol Chem. 2005; 280:37183–37194. [PubMed: 16115869]
16. Wen Y, Pinto JR, Gomes AV, Xu Y, Wang Y, Wang Y, et al. Functional Consequences of the Human Cardiac Troponin I Hypertrophic Cardiomyopathy Mutation R145G in Transgenic Mice. J Biol Chem. 2008; 283:20484–20494. [PubMed: 18430738]
17. Sanbe A, James J, Tuzcu V, Nas S, Martin L, Gulick J, et al. Transgenic rabbit model for human troponin I-based hypertrophic cardiomyopathy. Circulation. 2005; 111:2330–2338. [PubMed: 15867176]
18. Knollmann BC, Blatt SA, Horton K, de Freitas F, Miller T, Bell M, et al. Inotropic stimulation induces cardiac dysfunction in transgenic mice expressing a troponin T (I79N) mutation linked to familial hypertrophic cardiomyopathy. J Biol Chem. 2001; 276:10039–10048. [PubMed: 11113119]
19. Baudenbacher F, Schober T, Pinto JR, Sidorov VY, Hilliard F, Solaro RJ, et al. Myofilament Ca2+ sensitization causes susceptibility to cardiac arrhythmia in mice. J Clin Invest. 2008; 118:3893–3903. [PubMed: 19033660]
20. Ho CY, Lopez B, Coelho-Filho OR, Lakdawala NK, Cirino AL, Jarolim P, et al. Myocardial fibrosis as an early manifestation of hypertrophic cardiomyopathy. N Engl J Med. 2010; 363:552–563. [PubMed: 20818890]
21. Maron BJ, Towbin JA, Thiene G, Antzelevitch C, Corrado D, Arnett D, et al. Contemporary definitions and classification of the cardiomyopathies: an American Heart Association Scientific Statement from the Council on Clinical Cardiology, Heart Failure and Transplantation Committee; Quality of Care and Outcomes Research and Functional Genomics and Translational Biology Interdisciplinary Working Groups; and Council on Epidemiology and Prevention. Circulation. 2006; 113:1807–1816. [PubMed: 16567565]
22. Pinto JR, Reynaldo DP, Parvatiyar MS, Dweck D, Liang J, Jones MA, et al. Strong cross-bridges potentiate the Ca(2+) affinity changes produced by hypertrophic cardiomyopathy cardiac troponin C mutants in myofilaments: a fast kinetic approach. J Biol Chem. 2011; 286:1005–1013. [PubMed: 21056975]
23. Albury AN, Swindle N, Swartz DR, Tikunova SB. Effect of hypertrophic cardiomyopathy-linked troponin C mutations on the response of reconstituted thin filaments to calcium upon troponin I phosphorylation. Biochemistry. 2012; 51:3614–3621. [PubMed: 22489623]
24. Miller T, Szczesna D, Housmans PR, Zhao J, de Freitas F, Gomes AV, et al. Abnormal contractile function in transgenic mice expressing a familial hypertrophic cardiomyopathy-linked troponin T (I79N) mutation. J Biol Chem. 2001; 276:3743–3755. [PubMed: 11060294]
25. Li Y, Charles PY, Nan C, Pinto JR, Wang Y, Liang J, et al. Correcting diastolic dysfunction by Ca2+ desensitizing troponin in a transgenic mouse model of restrictive cardiomyopathy. J Mol Cell Cardiol. 2010; 49:402–411. [PubMed: 20580639]
26. Alves ML, Dias FA, Gaffin RD, Simon JN, Montminy EM, Biesiadecki BJ, et al. Desensitization of myofilaments to Ca2+ as a therapeutic target for hypertrophic cardiomyopathy with mutations in thin filament proteins. Circ Cardiovasc Genet. 2014; 7:132–143. [PubMed: 24585742]
27. Schober T, Huke S, Venkataraman R, Gryshchenko O, Kryshtal D, Hwang HS, et al. Myofilament Ca sensitization increases cytosolic Ca binding affinity, alters intracellular Ca homeostasis, and causes pause-dependent Ca-triggered arrhythmia. Circ Res. 2012; 111:170–179. [PubMed: 22647877]
28. Davis J, Yasuda S, Palpant NJ, Martindale J, Stevenson T, Converso K, Metzger JM. Diastolic dysfunction and thin filament dysregulation resulting from excitation-contraction uncoupling in a

Author Manuscript Author Manuscript Author Manuscript Author Manuscript

mouse model of restrictive cardiomyopathy. J Mol Cell Cardiol. 2012; 53:446–457. [PubMed: 22683325]

29. Gaffin RD, Pena JR, Alves MS, Dias FA, Chowdhury SA, Heinrich LS, et al. Long-term rescue of a familial hypertrophic cardiomyopathy caused by a mutation in the thin filament protein, tropomyosin, via modulation of a calcium cycling protein. J Mol Cell Cardiol. 2011; 51:812–820. [PubMed: 21840315]
30. Wang W, Barnabei MS, Asp ML, Heinis FI, Arden E, Davis J, et al. Noncanonical EF-hand motif strategically delays Ca2+ buffering to enhance cardiac performance. Nat Med. 2013; 19:305–312. [PubMed: 23396207]
31. Sequeira V, Wijnker PJ, Nijenkamp LL, Kuster DW, Najafi A, Witjas-Paalberends ER, et al. Perturbed length-dependent activation in human hypertrophic cardiomyopathy with missense sarcomeric gene mutations. Circ Res. 2013; 112:1491–1505. [PubMed: 23508784]
32. Neumann J. Altered phosphatase activity in heart failure, influence on Ca2+ movement. Basic Res Cardiol. 2002; 97(Suppl 1):I91–I95. [PubMed: 12479241]

Author Manuscript Author Manuscript Author Manuscript Author Manuscript

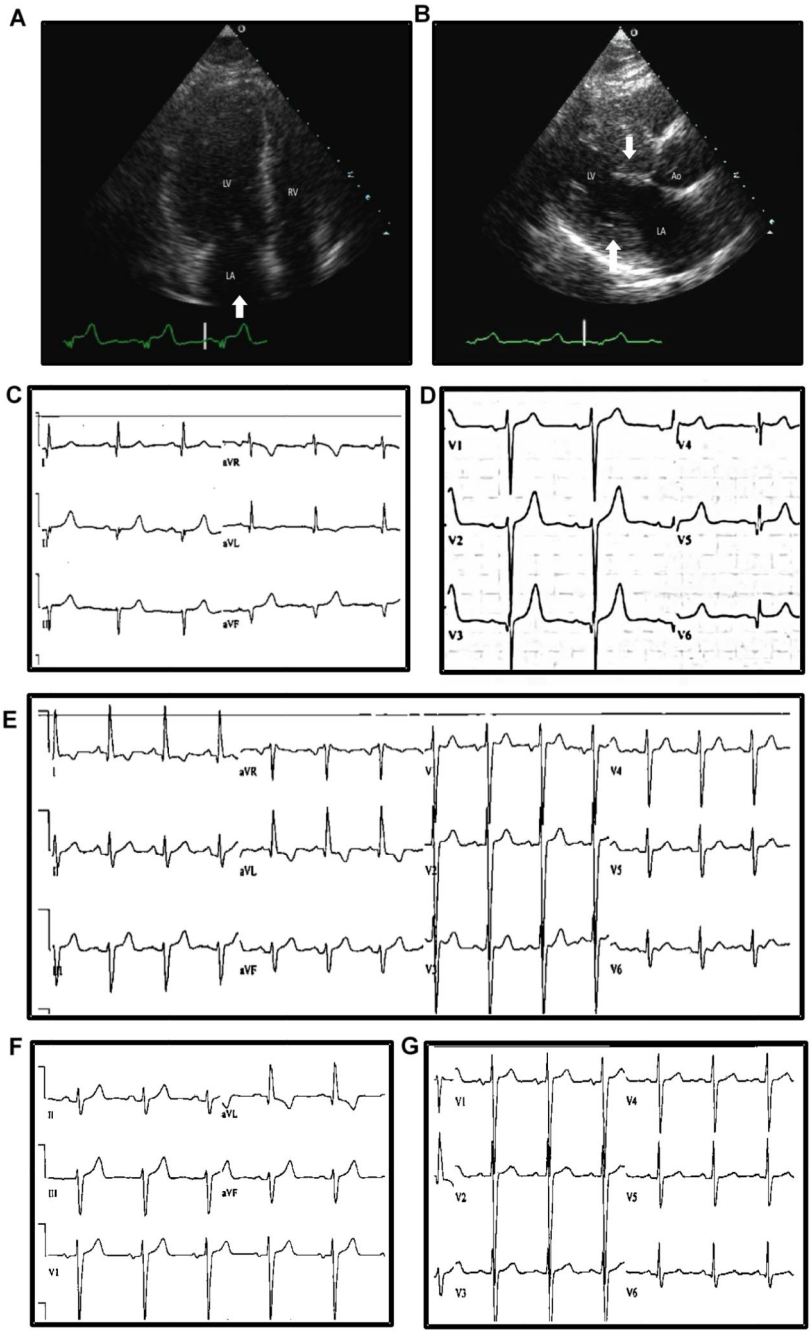

Figure 1.

Echo- and electro-cardiograms of the TNNC1-A8V patient. **A)** ECHO image from apical 4-chamber showing mild to moderate left-atrial enlargement (white arrow); **B)** ECHO image from parasternal long axis showing basal to mid-anteroseptal and posterior wall hypertrophy (white arrows) as an indication of concentric left-ventricle hypertrophy. LV = left ventricle; RV = right ventricle; LA = left atria; Ao = aorta. **C-G)** Electrocardiogram tracing from patient showing sinus rhythm, pathological Q-waves suggesting prior ischemia or

Author Manuscript Author Manuscript Author Manuscript Author Manuscript

hypertrophic cardiomyopathy **(C-F),** increased QRS amplitude suggesting left-ventricular hypertrophy (**E and G**).

Author Manuscript Author Manuscript Author Manuscript Author Manuscript

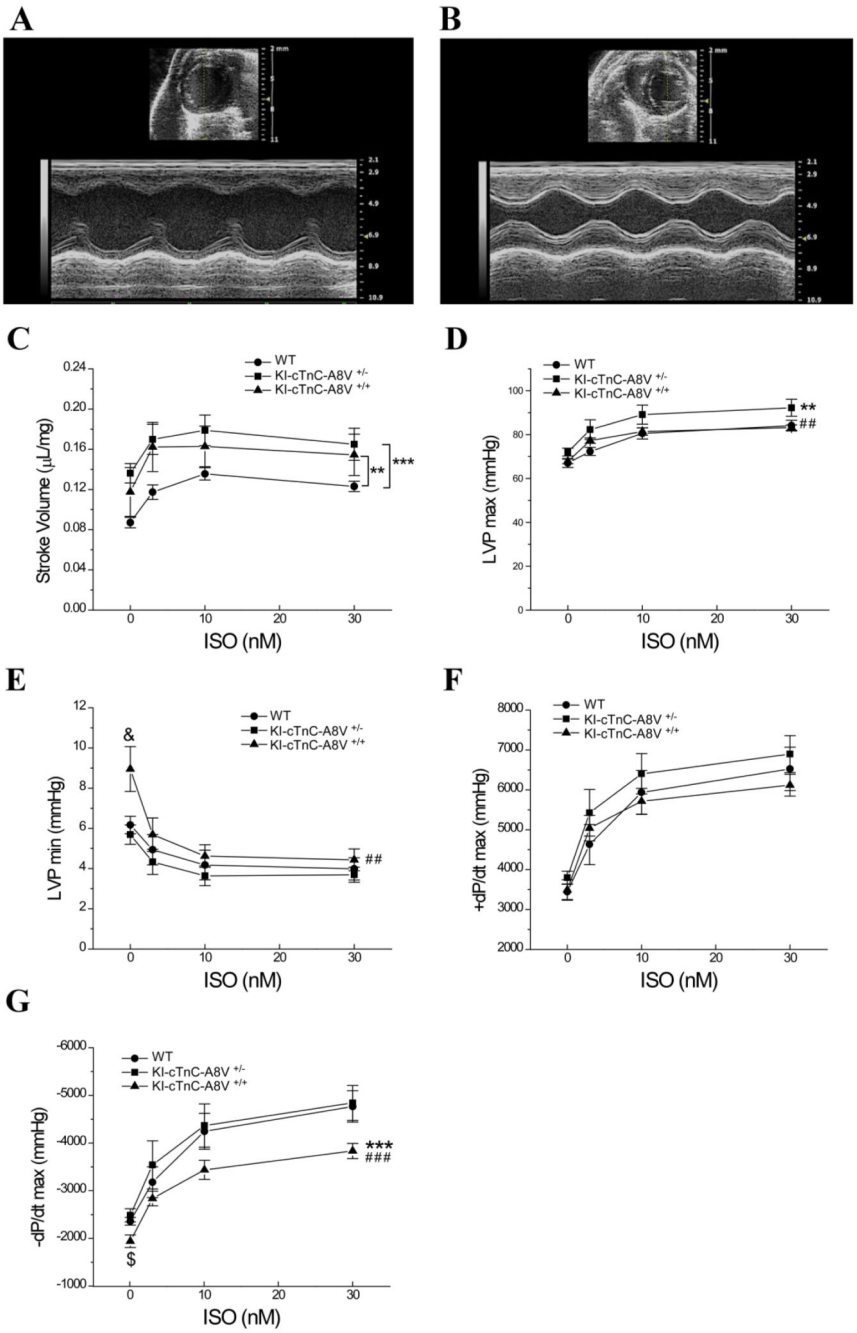

Figure 2.

Echocardiography and *ex-vivo* working heart function of the KI-TnC-A8V mice. A representative ECHO image of the left ventricle is shown in **A)** from a 14m WT mouse and in **B)** from a 14m KI-TnC-A8V$^{+/+}$ mouse. The response to β-adrenergic stimulation in e*x-vivo* working heart function in 12-13m mice is shown in **C)** Stroke volume normalized to the heart weight; **D)** LVP_{max} (maximal left-ventricular pressure); **E)** LVP_{min} (minimal left-ventricular pressure); **F)** +dP/dt (rate of rise of left-ventricular pressure); **G)** -dP/dt (rate of fall of left-ventricular pressure). ISO = isoproterenol. Data are shown as mean ± S.E., n = 5

Author Manuscript Author Manuscript Author Manuscript Author Manuscript

mice. **P<0.01 and ***P<0.001 KI *vs* WT; $^{\#\#}$P<0.01 and $^{\#\#\#}$P<0.001 KI-TnC-A8V$^{+/+}$ *vs* KI-TnC-A8V$^{+/-}$ using two-way ANOVA with Tukey adjustment. $^{\&}$P<0.05 KI-TnC-A8V$^{+/+}$ *vs* KI-TnC-A8V$^{+/-}$ and $^{\$}$P<0.05 KI-TnC-A8V$^{+/+}$ *vs* WT and KI-TnC-A8V$^{+/-}$ without ISO treatment using one-way ANOVA with Tukey adjustment.

Author Manuscript Author Manuscript Author Manuscript Author Manuscript

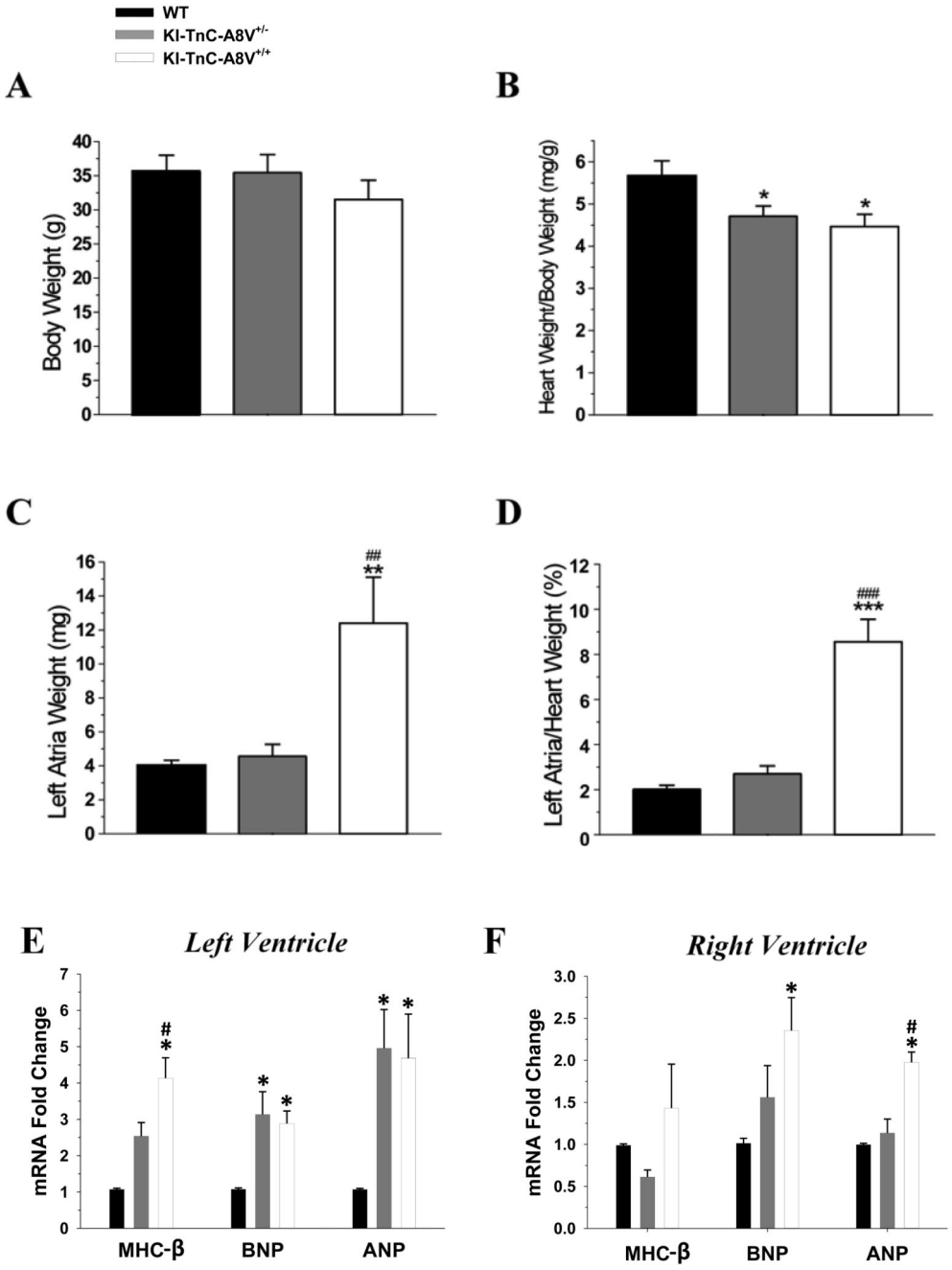

Figure 3.

Heart weight and hypertrophic cardiomyopathy gene-expression profile in KI-TnC-A8V mice. **A)** Shows the body weight; **B)** the ratio heart weight/body weight; **C)** the left atria weight; and **D)** the ratio left atria/heart weight. **A-D** are data from 12-13m mice. Data are shown as mean ± S.E., n = 5 mice. *P<0.05, **P<0.01 and *** P<0.001 KI *vs* WT; ##P<0.01 and ###P<0.001 KI-TnC-A8V$^{+/+}$ *vs* KI-TnC-A8V$^{+/-}$. **E** and **F)** The mRNA expression levels of cardiac hypertrophic markers in 16-18m mice. ANP, atrial natriuretic peptide; BNP, brain natriuretic peptide and MHCβ, myosin heavy chain isoform β. Data are

shown as mean ± S.E., n = 6 mice. *p<0.05 KI *vs* WT; #p<0.05 KI-TnC-A8V$^{+/+}$ *vs* KI-TnC-A8V$^{+/-}$.

Author Manuscript Author Manuscript Author Manuscript Author Manuscript

Author Manuscript Author Manuscript Author Manuscript Author Manuscript

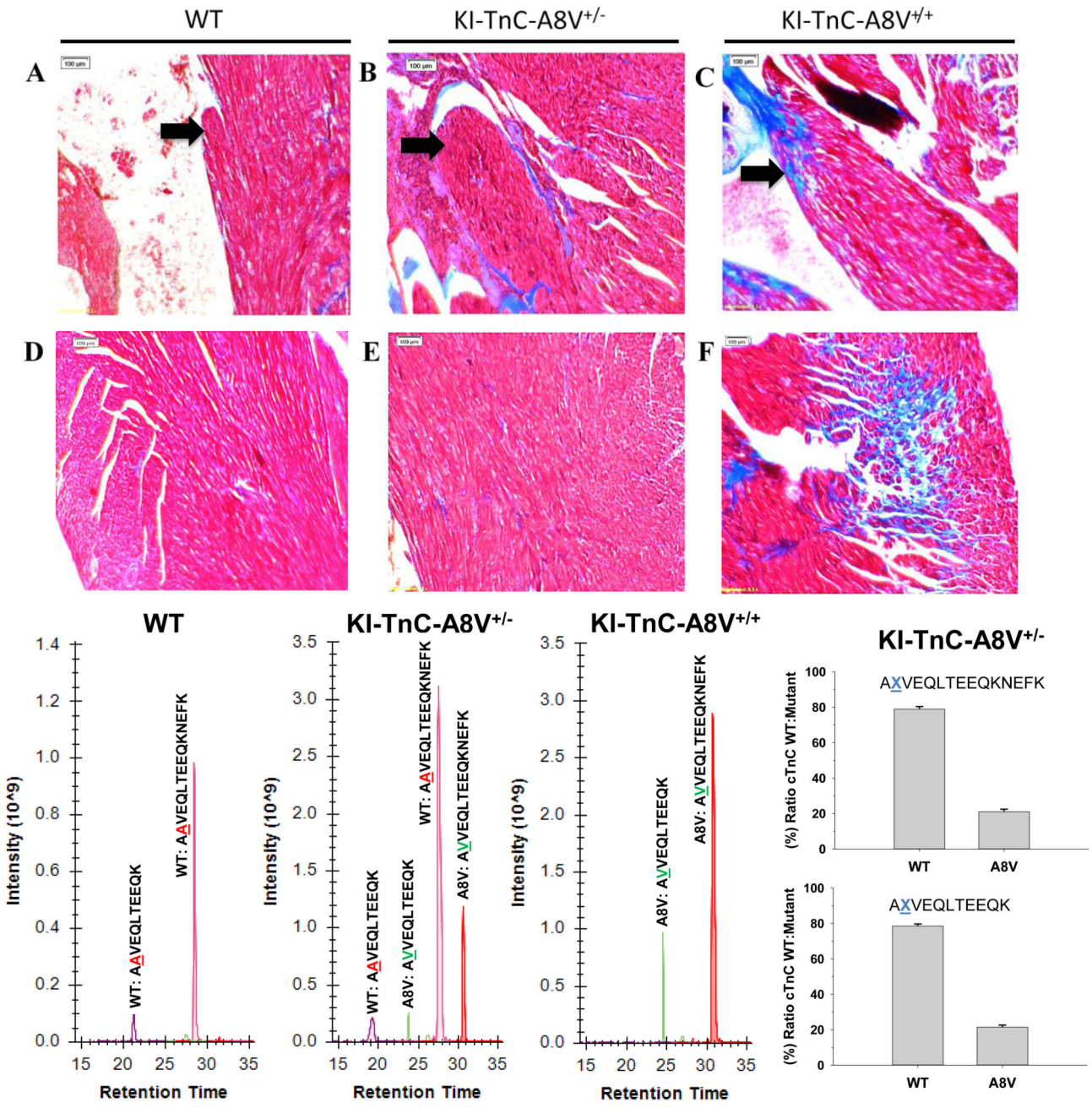

Figure 4.

Histopathological analysis of KI-TnC-A8V mouse hearts at 16-18 months of age. Representative Masson trichrome stained sections were imaged at 10X magnification. In panels **A-C**) the black arrows indicate the location of papillary muscles. Papillary muscle hypertrophy can be seen in KI-TnC-A8V$^{+/-}$ and KI-TnC-A8V$^{+/+}$ mouse hearts. Evidence of papillary muscle hypertrophy can also be seen at lower magnification in Supplemental Figure 2A-C. In panels **E-F)** interstitial fibrosis can be seen in heart sections obtained from the same group of mice. **G)** the retention time of the cTnC peptides separated by liquid

chromatography mass spectrometry. The graphs show the ratio cTnC A8V:WT in the KI-TnC-A8V$^{+/-}$ hearts quantified by the abundance of 15 and 11 amino acid peptides. n = 3.

Author Manuscript Author Manuscript Author Manuscript Author Manuscript

Author Manuscript Author Manuscript Author Manuscript Author Manuscript

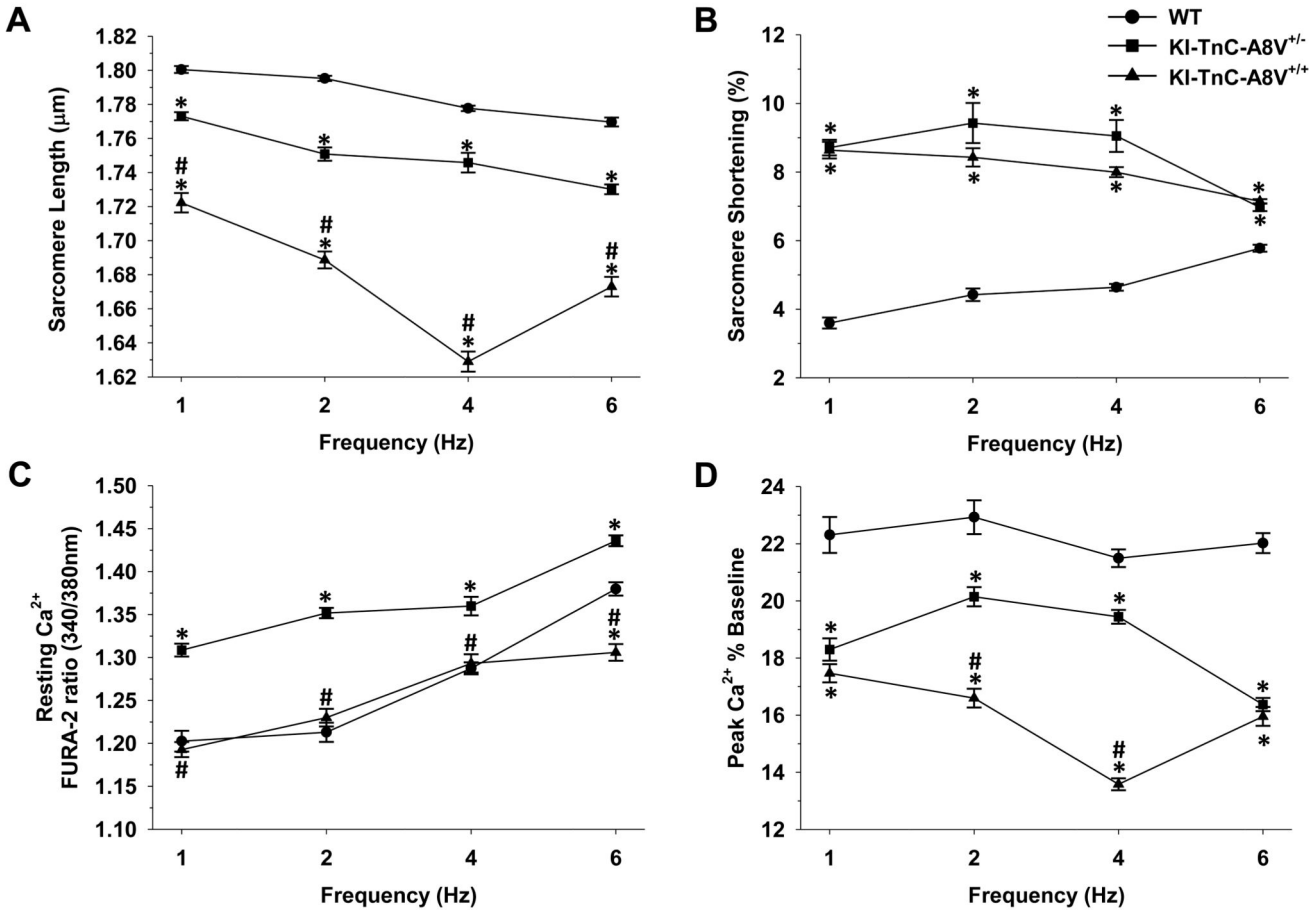

Figure 5.

Sarcomere length (SL) and intracellular Ca^{2+} levels in KI-TnC-A8V intact cardiomyocytes at different frequencies of stimulation. **A)** SL is measured under resting conditions; **B)** Percentage of SL shortening; **C)** Diastolic intracellular Ca^{2+} levels; **D)** Ca^{2+} amplitude is represented as the percentage of increase above diastolic intracellular Ca^{2+} levels in cardiomyocytes obtained from 3m-old mice. Data are shown as mean ± S.E., n = 3-4 mice. $^{*}p<0.05$ KI *vs* WT; $^{\#}p<0.05$, KI-TnC-A8V$^{+/+}$ *vs* KI-TnC-A8V$^{+/-}$ at the same frequency of stimulation. The values for each point are presented in Supplemental Table 1.

Author Manuscript Author Manuscript Author Manuscript Author Manuscript

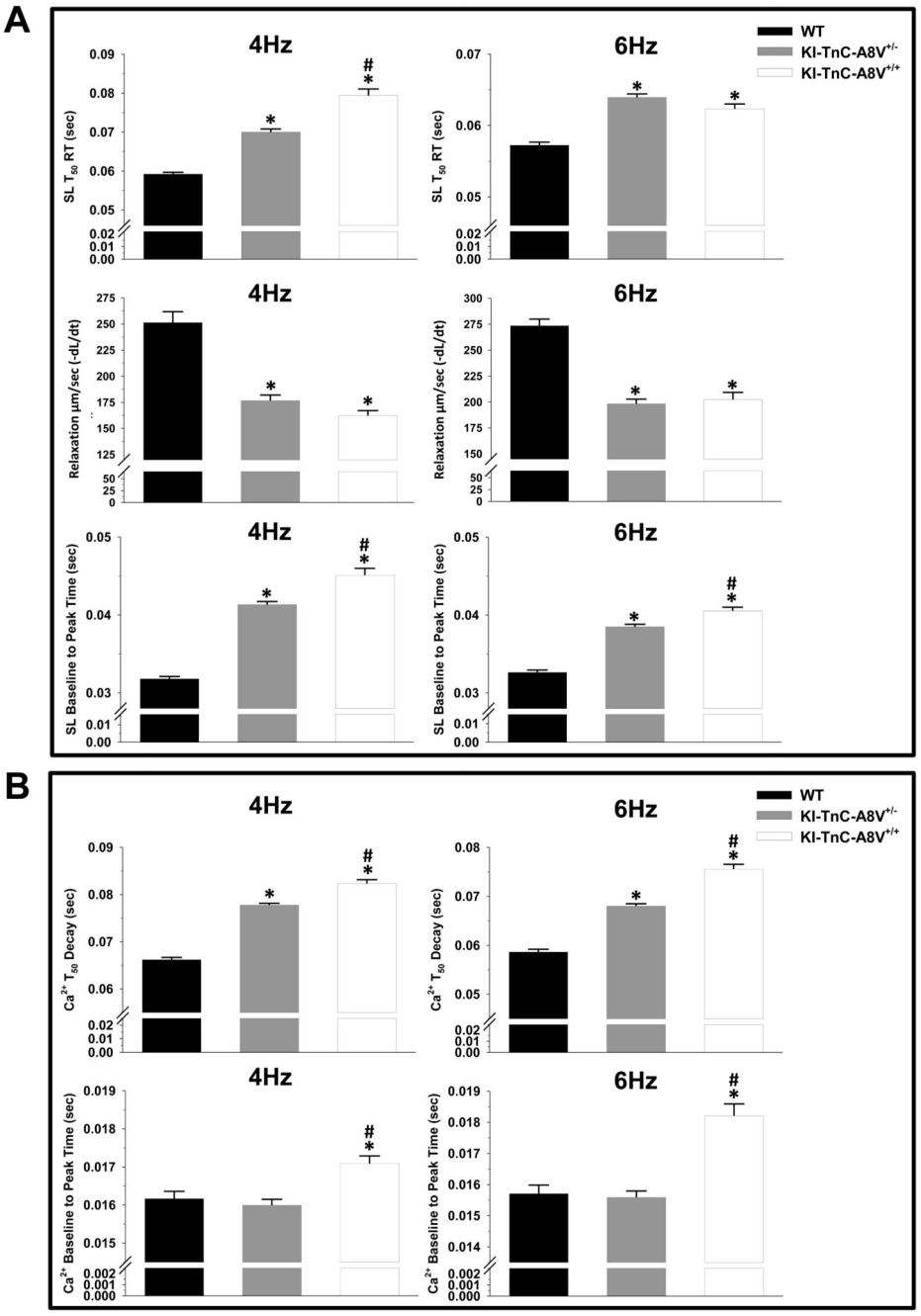

Figure 6.

Kinetics of contractility and Ca^{2+} transients in KI-TnC-A8V intact cardiomyocytes electrically stimulated at 4 and 6Hz. **A**) Time for the sarcomere length (SL) to return to 50% of baseline (RT, relaxation time); the rate of cell re-lengthening (−dL/dt); and time for SL shortening to achieve the peak value. **B**) Time for intracellular Ca^{2+} to return to 50% of baseline; and the time for intracellular $Ca^{2+}$to achieve peak during systole. Data are shown as mean ± S.E., n = 3-4 mice. $^{*}p<0.05$ KI *vs* WT; $^{\#}p<0.05$, KI-TnC-A8V$^{+/+}$ *vs* KI-TnC-A8V$^{+/-}$. The values for each point are presented in Supplemental Table 2.

Author Manuscript Author Manuscript Author Manuscript Author Manuscript

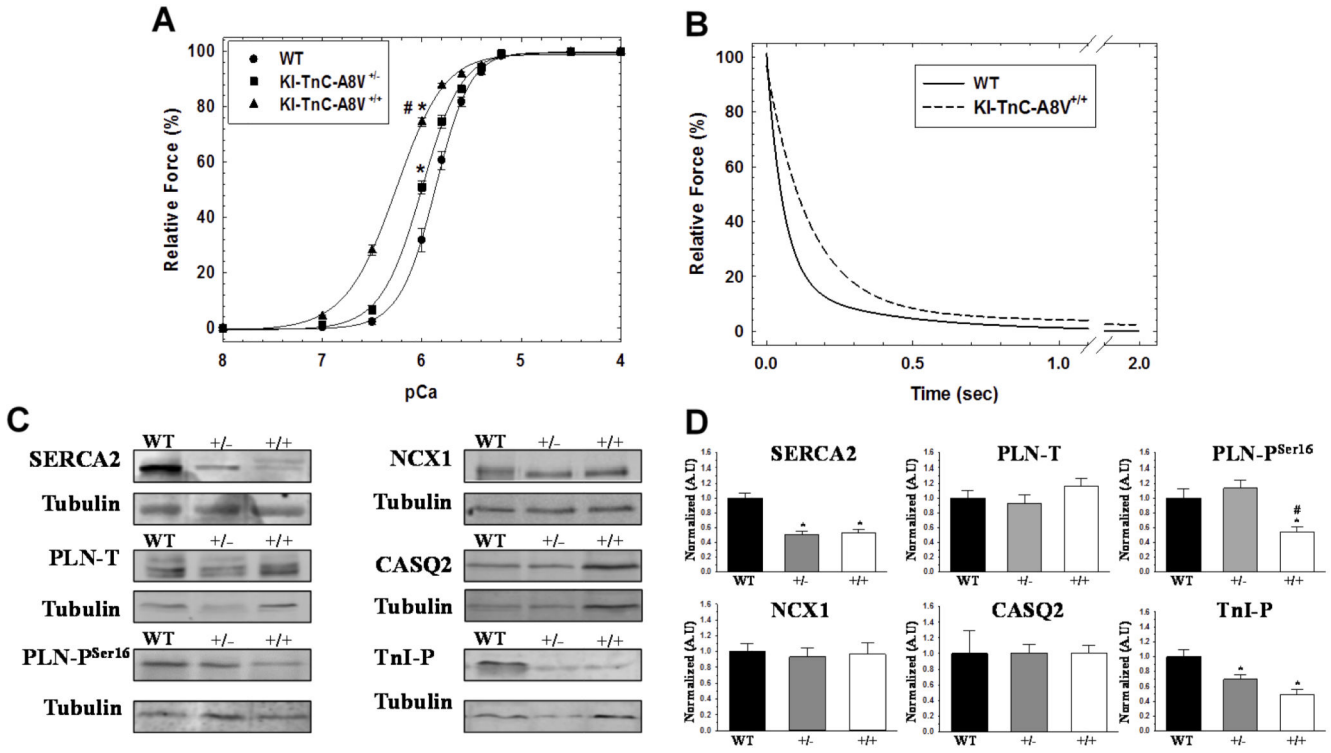

Figure 7.

The Ca^{2+} sensitivity of force development and rate of relaxation in papillary skinned fibers and immunoblots of Ca^{2+}-handling proteins in KI-TnC-A8V hearts. **A)** The Ca^{2+} dependence of force generation in cardiac skinned fibers from 4m-old mice. Data are shown as mean ± S.E., n = 9-11. $^{*}p<0.05$ KI *vs* WT; $^{\#}p<0.05$ KI-TnC-A8V$^{+/+}$ *vs* KI-TnC-A8V$^{+/-}$. **B)** A representative tracing measuring the rate of relaxation in cardiac skinned fibers investigated by Diazo-2 upon flash photolysis. The amplitudes (*A*, %) and rate constants (*k*, s^{-1}) obtained from 4m-old mice were as follows; WT: A_1 = 83.82 ± 2.06, k_1 = 15.48 ± 0.9, A_2 = 14.56 ± 2.47 and k_2 = 2.01 ± 0.53; KI-TnC-A8V$^{+/+}$: A_1 = 84.24 ± 5.06, k_1 = 9.42 ± 0.84, A_2 = 14.28 ± 4.36 and k_2 = 0.75 ± 0.18. k_1 and k_2 are statistically different between WT and KI-TnC-A8V$^{+/+}$ ($p<0.05$). The $t_{1/2}$ (ms) of skinned-fiber relaxation was also statistically different between WT (55.62 ± 4.25) and KI-TnC-A8V$^{+/+}$ (82.86 ± 6.78), n = 8-11. **C)** Representative immunoblots for the detection of SERCA2, PLN-T, phosphorylated PLN at serine 16 (PLN-P^{Ser16}), NCX1, CASQ2 and phosphorylated cTnI at serines 23, 24 (cTnI-P) in the left ventricle of 9m old WT, KI-TnC-A8V$^{+/-}$ (+/−) and KI-TnC-A8V$^{+/+}$ (+/+) mice. For all experiments, tubulin was used as an internal control. **D)** Quantification of the protein expression and phosphorylation levels. Data are shown as mean ± S.E., n = 6 mice. $^{*}p<0.05$ KI *vs* WT; $^{\#}p<0.05$ KI-TnC-A8V$^{+/+}$ *vs* KI-TnC-A8V$^{+/-}$.

Author Manuscript Author Manuscript Author Manuscript Author Manuscript

Circ Cardiovasc Genet. Author manuscript; available in PMC 2016 October 01.

Table 1

Summary of echocardiographic data from wild-type (WT) and both heterozygous (HT) and homozygous (HM) KI-TnC-A8V mice

	3 months			9 months			14 months		
	WT (n=10)	**HT (n=12)**	**HM (n=14)**	**WT (n=11)**	**HT (n=11)**	**HM (n=8)**	**WT (n=14)**	**HT (n=8)**	**HM (n=12)**
ECHO Parameter									
HR (bpm)	458 ± 6	448 ± 12	447 ± 8	481 ± 10	448 ± 15	448 ± 22	462 ± 14	445 ± 11	435 ± 15
EDV (ul)	55 ± 4	51 ± 6	37 ± 2†‡	53 ± 6	55 ± 5	35 ± 4*‡	69 ± 6	49 ± 3†	43 ± 3†
ESV (ul)	17 ± 3	14 ± 2	8 ± 1*	15 ± 3	18 ± 3	7 ± 2*‡	19 ± 3	10 ± 2*	10 ± 2*
LVEDD (mm)	3.6 ± 0.1	3.4 ± 0.1	3.1 ± 0.1†‡	3.5 ± 0.2	3.6 ± 0.1	3.0 ± 0.1*‡	3.9 ± 0.1	3.4 ± 0.1*	3.2 ± 0.1†
LVESD (mm)	2.1 ± 0.1	1.9 ± 0.1	1.6 ± 0.1†	2.1 ± 0.1	2.2 ± 0.1	1.4 ± 0.1†§	2.3 ± 0.2	1.8 ± 0.1*	1.7 ± 0.1*
EF (%)	71 ± 3	73 ± 3	78 ± 3*	73 ± 3	70 ± 3	82 ± 3*‡	74 ± 3	78 ± 3	77 ± 4
AET (ms)	50 ± 3	54 ± 2	52 ± 2	42 ± 2	47 ± 2	47 ± 3	41 ± 2	39 ± 3	50 ± 2*‡
DecelTime (ms)	15 ± 2	14 ± 1	14 ± 1	11 ± 1	14 ± 1*	16 ± 2*	15 ± 1	14 ± 1	13 ± 1
IVRT (ms)	20 ± 1	20 ± 1	27 ± 2†§	20 ± 2	21 ± 1	31 ± 3†§	19 ± 2	25 ± 3	27 ± 2*
IVCT (ms)	17 ± 2	18 ± 2	14 ± 1	23 ± 2	22 ± 2	16 ± 1†‡	22 ± 3	24 ± 4	15 ± 1*‡
MV E/A	1.6 ± 0.2	1.6 ± 0.1	1.1 ± 0.5*‡	1.6 ± 0.2	1.5 ± 0.1	1.0 ± 0.1*‡	1.1 ± 0.1	1.0 ± 0.1	1.1 ± 0.1
RWT (%)	51 ± 5	61 ± 3*	71 ± 1†§	53 ± 5	62 ± 3*	69 ± 5†‡	46 ± 6	65 ± 7†	65 ± 5†
LV mass (mg)	145 ± 14	149 ± 10	103 ± 6*‡	166 ± 11	150 ± 13	112 ± 10*	146 ± 8	148 ± 16	134 ± 11

Data are mean ± SEM. HR, heart rate; SV, stroke volume; CO, cardiac output; EDV, edn diastolic volume; ESV, end systolic volume; EF, ejection fraction; FS, fractional shortening; LV; left ventricular; EDD, end diastolic diameter; ESD, end systolic diameter; AET, aortic ejection time; DecelTime, deceleration time; IVRT, isovolumetric relaxation time; IVCT, isovolumetric contraction time; MV, mitral valve; E, early peak flow velocity; A, atrial peak flow velocity; RWT, relative wall thickness. RWT was calculated as follows: ((2×PWTd)/LVEDD)×100). PWTd=posterior wall thickness during diastole. ANOVA with LSD post hoc test

*p<0.05,

†p<0.01 HT or HM *vs* WT within age timepoint;

‡p<0.05,

§p<0.01 HM *vs* HT within age timepoint.